Facile Preparation of Hierarchically Porous Carbon Monoliths with Well-Ordered Mesostructures

ARTICLE *in* CHEMISTRY OF MATERIALS · DECEMBER 2006

Impact Factor: 8.35 · DOI: 10.1021/cm061531a

3 AUTHORS:

Xiqing Wang
Nanotek Instruments, Inc.
55 PUBLICATIONS **2,237** CITATIONS
SEE PROFILE

Krassimir N. Bozhilov
University of California, Riverside
84 PUBLICATIONS **2,288** CITATIONS
SEE PROFILE

Pingyun Feng
University of California, Riverside
200 PUBLICATIONS **12,562** CITATIONS
SEE PROFILE

Facile Preparation of Hierarchically Porous Carbon Monoliths with Well-Ordered Mesostructures

Xiqing Wang,[†] Krassimir N. Bozhilov,[‡] and Pingyun Feng*,[†]

Department of Chemistry, and Central Facility for Advanced Microscopy and Microanalysis, University of California, Riverside, California 92521

Received July 3, 2006. Revised Manuscript Received October 10, 2006

By integration of gel casting with chemical vapor deposition (CVD), hierarchically porous carbon monoliths with either hexagonal or cubic mesostructures are prepared starting from well-ordered mesoporous silica powders (SBA-15 and KIT-6). Powdery silica particles are first fused together to form silica monoliths by the gel-casting method. Furfuryl alcohol at various concentrations in trimethylbenzene is used as carbon precursor. The use of low concentration of furfuryl alcohol, together with a secondary loading of carbon by the CVD method, allows an additional level of control over the hierarchical porosity of carbon monoliths. In addition, monolithic carbon materials with connected hexagonally packed nanopipes are fabricated for the first time here from large-pore SBA-15. The carbon monoliths exhibit macroporosity, well-ordered mesoporosity with either hexagonal or bicontinuous cubic symmetry, and controlled microporosity. The method described can be extended to prepare other types of carbon monoliths with different symmetries when appropriate silica templates with a connected pore system (e.g., MCM-48, SBA-16, and NaY) are applied.

Introduction

Ordered mesoporous carbons have attracted considerable attention in the past few years due to their uniform pore size, high surface area, and large pore volume.[1] Ordered mesoporous silicas[2] with connected pore systems are used as the hard templates for the synthesis. The synthetic technique, called "nanocasting", involves impregnation of silica templates with an appropriate carbon source, carbonization of carbon precursor, and subsequent removal of silica.[3] The resulting carbons are inverse replicas of ordered mesoporous silicas. Since the first successful example of using MCM-48 to make carbon replica, named CMK-1[3a] (or SNU-1[3b]), ordered mesoporous carbons with various structures[4] have been reported from different silica templates, e.g., CMK-3 from SBA-15[5] and CMK-8 from KIT-6.[6] In addition, ordered carbon consisting of 2D hexagonal nanopipes (CMK-5) can be made through the surface-templating approach from SBA-15.[7]

To date, most work has been focused on the synthesis of carbons with new structures,[8] on the use of new carbon precursors,[9] or on the control of pore size,[10] and there are only a few reports[11−13] on the control of macroscopic morphology. Monoliths are especially important among different morphologies because they are essential for some practical applications, such as monolithic high-performance liquid chromatography (HPLC). Carbon monoliths can be prepared by using monolithic mesoporous silica[14] solid

* To whom correspondence should be addressed. Fax: 951-827-4713. E-mail: pingyun.feng@ucr.edu.
† Department of Chemistry.
‡ Central Facility for Advanced Microscopy and Microanalysis.

(1) (a) Ryoo, R.; Joo, S. H.; Kruk, M.; Jaroniec, M. *Adv. Mater.* **2001**, *13*, 677. (b) Lee, J.; Han, S.; Hyeon, T. *J. Mater. Chem.* **2004**, *14*, 478.
(2) (a) Kresge, C. T.; Leonowicz, M. E.; Roth, W. J.; Vartuli, J. C.; Beck, J. S. *Nature* **1992**, *359*, 710. (b) Huo, Q.; Margolese, D. I.; Ciesla, U.; Demuth, D. G.; Feng, P.; Gier, T. E.; Sieger, P.; Firouzi, A.; Chmelka, B. F.; Schth, F.; Stucky, G. D. *Chem. Mater.* **1994**, *6*, 1176. (c) Huo, Q.; Margolese, D. I.; Stucky, G. D. *Chem. Mater.* **1996**, *8*, 1147.
(3) (a) Ryoo, R.; Joo, S. H.; Jun, S. *J. Phys. Chem. B* **1999**, *103*, 7743. (b) Lee, J.; Yoon, S.; Hyeon, T.; Oh, S. M.; Kim, K. B. *Chem. Commun.* **1999**, 2177.
(4) Ryoo, R.; Joo, S. H.; Ju, S.; Tsubakiyama, T.; Terasaki, O. *Stud. Surf. Sci. Catal.* **2004**, *72*, 59.
(5) Jun, S.; Joo, S. H.; Ryoo, R.; Kruk, M.; Jaroniec, M.; Liu, Z.; Ohsuna, T.; Terasaki, O. *J. Am. Chem. Soc.* **2000**, *122*, 10712.
(6) Kleitz, F.; Choi, S. H.; Ryoo, R. *Chem. Commun.* **2003**, 2136.
(7) Joo, S. H.; Choi, S. J.; Oh, I.; Kwak, J.; Liu, Z.; Terasaki, O.; Ryoo, R. *Nature* **2001**, *412*, 169.
(8) (a) Kim, S.-S.; Pinnavaia, T. J. *Chem. Commun.* **2001**, 2418. (b) Lee, J.; Sohn, K.; Hyeon, T. *J. Am. Chem. Soc.* **2001**, *123*, 5146. (c) Kim, T.-W.; Ryoo, R.; Gierszal, K. P.; Jaroniec, M.; Solovyov, L.; Sakamoto, Y.; Terasaki, O. *J. Mater. Chem.* **2005**, *15*, 1560.
(9) (a) Yoon, S. B.; Kim, J. Y.; Yu. J.-S. *Chem. Commun.* **2001**, 559. (b) Kim, T.-W.; Park, I.-S.; Ryoo, R. *Angew. Chem., Int. Ed.* **2003**, *42*, 4375. (c) Kim, C. H.; Lee, D.-K.; Pinnavaia, T. J. *Langmuir* **2004**, *20*, 5157. (d) Kruk, M.; Dufour, B.; Celer, E. B.; Kowalewski, T.; Jaroniec, M.; Matyjaszewski, K. *J. Phys. Chem. B* **2005**, *109*, 9216.
(10) (a) Lee, J.-S.; Joo, S. H.; Ryoo, R. *J. Am. Chem. Soc.* **2002**, *124*, 1156. (b) Fuertes, A. B. *Microporous Mesoporous Mater.* **2004**, *67*, 273.
(11) Rod: Yu, C.; Fan, J.; Tian, B.; Zhao, D.; Stucky, G. D. *Adv. Mater.* **2002**, *14*, 1742.
(12) Spheres: (a) Fuertes, A. B. *J. Mater. Chem.* **2003**, *13*, 3085. (b) Hampsey, J. E.; Hu, Q.; Wu, Z.; Rice, L.; Pang, J.; Lu, Y. *Carbon* **2005**, *43*, 2977. (c) Hampsey, J. E.; Hu, Q.; Rice, L.; Pang, J.; Wu, Z.; Lu, Y. *Chem. Commun.* **2005**, 3606.
(13) Film: Pang, J.; Li, X; Wang, D.; Wu, Z.; John, V. T.; Yang, Z.; Lu, Y. *Adv. Mater.* **2004**, *16*, 884.
(14) (a) Feng, P.; Bu, X.; Stucky, G. D.; Pine, D. J. *J. Am. Chem. Soc.* **2000**, *122*, 994. (b) Yang, H. F.; Shi, Q. H.; Tian, B. Z.; Xie, S. H.; Zhang, F. Q.; Yan, Y.; Tu, B.; Zhao, D. Y. *Chem. Mater.* **2003**, *15*, 536.

10.1021/cm061531a CCC: $33.50
Published on Web 12/19/2006

Scheme 1. Synthesis Procedure of Carbon Monoliths

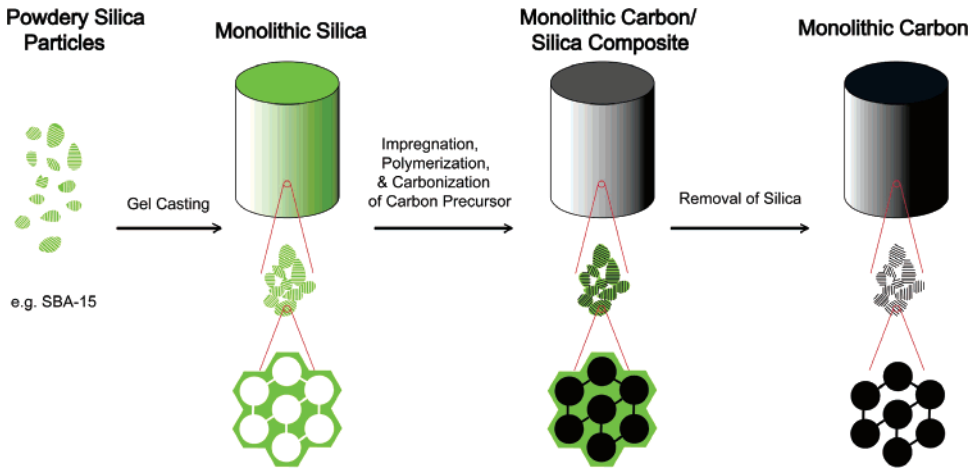

templates. At present, only microporous,[15] ordered mesoporous,[16] bimodal meso-macroporous,[17] and disordered carbon connected ordered mesoporous[18] carbon monoliths have been reported. However, there are no reports of hierarchically porous carbon monoliths composed of ordered mesoporous carbon. In addition, mesoporous silica monoliths in most of these studies are prepared directly from templated sol−gel processes, which often lead to a lower structural ordering at the mesoscale or are less versatile in terms of control of pore geometry and size compared to the synthesis of corresponding powdery forms.

In this paper, we report a unique combination of synthetic procedure for the preparation of carbon monoliths with hierarchically porous structures integrating macroporosity, ordered mesoporosity, and controlled microporosity, by starting from powdery mesoporous silicas. Silica monoliths are prepared by the polymerization-based gel-casting method from powdery mesoporous silica. By starting from powdery mesoporous silica, rather than the direct chemical synthesis of silica monoliths, very diverse types of silica templates with various pore geometries and sizes can be used with this method, making it possible to create carbon monoliths with a comparable diversity of pore geometries and sizes. The carbon mesostructures can be controlled by concentrations of carbon precursors, in combination with CVD in cases of low precursor concentrations. Such methods lead to the preparation of carbon monoliths constructed of both rod-type (e.g., CMK-3) and tube-type (e.g., CMK-5) carbon rods, in addition to the bicontinuous cubic structure.

Experimental Section

The synthesis procedure for preparation of monolithic porous silicas and carbons is shown in Scheme 1. Silica monoliths were made from powdery mesoporous silicas by the gel-casting method[19] in which acrylamide was polymerized to form a strong, cross-linked network filled with silica particles, followed by burning off of the polymer.

Reagents. Poly(ethylene oxide)−poly(propylene oxide)−poly(ethylene oxide) triblock copolymer Pluronic P123 ($EO_{20}PO_{70}EO_{20}$, M.W. = 5800 g/mol) was received from BASF as a gift. Tetraethyl orthosilicate (TEOS), furfuryl alcohol (FA), oxalic acid, hydrochloric acid (35−38 wt %), and hydrofluoric acid (48−51 wt %) were purchased from Acros-Fisher. 1,3,5-Trimethylbenzene (TMB), acrylamide, *N*,*N*′-methylene-bisacrylamide, and ammonium persulfate were obtained from Aldrich. Acetonitrile was received from EMD Chemicals.

Synthesis of Powdery Mesoporous Silicas. SBA-15 and KIT-6 were synthesized as follows. High-quality SBA-15 was prepared following Zhao et al.'s procedure[20] with a slight modification. In a large polypropylene bottle, 8 g of P123 was dissolved in a mixture of 40 g of concentrated HCl and 260 g of distilled water, followed by the addition of 17 g of TEOS with vigorous stirring for 15 min at 35 °C. The mixture was kept statically at the same temperature for 24 h and subsequently heated at 110 °C for another 24 h. Large-pore SBA-15 was synthesized using the same procedure but was heated at 130 °C instead of 110 °C for 24 h. Synthesis of KIT-6 was carried out from a starting composition of 0.017:1.2:1.31:1.83:195 P123:TEOS:BuOH:HCl:H_2O (in molar ratio).[21] After 8 g of P123 was dissolved in 288 g of distilled water and 15.8 g of concentrated HCl, 8 g of BuOH was added with vigorous stirring at 35 °C for 1 h. To the solution, 20.64 g of TEOS was added with stirring. The mixture was stirred at 35 °C for 24 h and then put in an oven at 110 °C for another 24 h under static conditions. All precipitates were filtered, washed with distilled water and ethanol, and calcined at 550 °C in air for 5 h. The resulting silica products were typically in the form of powders.

Fabrication of Silica Monolith. The mesoporous silica monoliths were made from powdery mesoporous silicas by the gel-casting method.[19] Typically, powdery mesoporous silicas (SBA-15 and KIT-6) were well-dispersed in an aqueous solution containing acrylamide (monomer), *N*,*N*′-methylene-bisacrylamide (cross-linker), and ammonium persulfate (initiator) by sonication for 20 min. The mass ratio of monomer, cross-linker, initiator, and water was 5:0.5:0.05:100. The resulting homogeneous mixture was transferred into a glass vial and then centrifuged at 6000 rpm for

(15) Han, B.-H.; Zhou, W.; Sayari, A. *J. Am. Chem. Soc.* **2003**, *125*, 3444.
(16) Yang, H.; Shi, Q.; Liu, X.; Xie, S.; Jiang, D.; Zhang, F.; Yu, C.; Tu, B.; Zhao, D. *Chem. Commun.* **2002**, 2842.
(17) (a) Taguchi, A.; Smått, J.-H.; Lindén, M. *Adv. Mater.* **2003**, *15*, 1209. (b) Lu, A.-H.; Smått, J.-H.; Backlunk, S.; Lindén, M. *Microporous Mesoporous Mater.* **2004**, *72*, 59. (c) Lu, A.-H.; Smått, J.-H.; Lindén, M. *Adv. Funct. Mater.* **2005**, *15*, 865. (d) Shi, Z.-G.; Feng, Y.-Q.; Xu, L.; Da, S.-L.; Zhang, M. *Carbon* **2003**, *41*, 2653.
(18) Wang, L.; Lin, S.; Lin, K.; Yin, C.; Liang, D.; Di, Y.; Fan, P.; Jiang, D.; Xiao, F.-S. *Microporous Mesoporous Mater.* **2006**, *85*, 136.
(19) Liang, C.; Dai, S.; Guiochon, G. *Chem. Commun.* **2002**, 2680.
(20) Zhao, D.; Feng, J.; Huo, Q.; Melosh, N.; Fredirckson, G. H.; Chemlka, B. F.; Stucky, G. D. *Science* **1998**, *279*, 548.
(21) Kim, T.-W.; Kleitz, F.; Paul, B.; Ryoo, R. *J. Am. Chem. Soc.* **2005**, *127*, 7601.

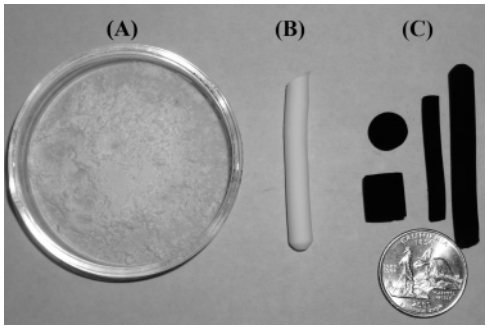

Figure 1. Photographs of (A) powdery mesoporous silica, (B) silica monolith, and (C) carbon monoliths with various diameters and lengths. Insert is a U.S. quarter coin with a size of 2.5 cm in diameter.

5 min. After removal of the upper solution, the glass vial was capped and put in an oven. Once the temperature was increased to 60 °C, the monomers were quickly polymerized to form a highly cross-linked hydrogel in which powdery mesoporous silicas were homogeneously incorporated. After polymerization for 2 h, the glass vial was left open and dried at 60 °C overnight under vacuum. The obtained gel cast faithfully took the shape of the glass vial and can be easily cut into desired shapes and lengths. The gel cast was further dried at 60 °C for 1−2 days. Finally, the polymer−silica composite was calcined at 700 °C for 10 h under air at a heating rate of 2.5 °C/min to burn off the polymer and to sinter the silica powder into a rigid monolith. The silica monoliths from powdery SBA-15 and KIT-6 are denoted as SBA-15M (SBA-15LM from large-pore SBA-15) and KIT-6M, respectively.

Preparation of Carbon Monolith. Typically, silica monolith was immersed into a trimethylbenzene (TMB) solution of furfuryl alcohol (FA) containing oxalic acid (OxA, molar ratio of FA/OxA = 250) overnight for complete wet impregnation. Polymerization of FA was performed at 60 and 85 °C each for 24 h where OxA acted as a catalyst. After being cured at 150 °C under N_2 for 3 h in a quartz furnace, the impregnated sample was heated at a rate of 2 °C/min to 850 °C, and the pyrolysis was carried out at the same temperature for 4 h under N_2. In some experimental runs, the thus-obtained carbon−silica composites were further loaded with more carbon by the chemical vapor deposition (CVD) method[27] to improve the structural integrity. In the later cases, N_2-saturated acetonitrile was passed through the furnace at a flow rate of 100 cm^3/min when the composites were heated at 750−900 °C, at a heating rate of 10 °C/min, for 3 h. Monolithic carbons were obtained after removal of silica by HF, washed with copious water, and dried at 80 °C under vacuum.

Characterization. Powder X-ray diffraction (XRD) patterns were recorded on a Bruker D8 Advance diffractometer with Cu Kα radiation (40 kV, 40 mA). N_2 sorption analysis was performed on a Micromeritics ASAP2010 volumetric adsorption analyzer at 77 K. Prior to the measurement, the samples were degassed at 150 °C for 4 h. The specific surface area was calculated using the BET method from the nitrogen adsorption data in the relative range (P/P_0) of 0.04−0.20. The total pore volume was determined from the amount of N_2 uptake at P/P_0 of 0.99. The microporosity of silica templates was deduced from the *t* plots. The primary pore volume (pore size <5 nm) and the external surface area of porous carbons were obtained using the high-resolution α_s plot method. Nitrogen adsorption data on nongraphitized carbon black (Cabot BP 280, S_{BET} = 40.2 m^2/g)[22] was used as a reference to construct the α_s plots. SEM and TEM images were recorded on a Philips XL30 scanning electron microscope and a Philips CM300 transmission electron microscope, respectively. Mechanical strength tests were carried out by piling metal pieces on the monolithic rod (1 cm in diameter) until it broke or cracked (see the Supporting Information). The compressive strength of monolithic materials was calculated by dividing the weight of metal pieces over the cross area of the rod.[23]

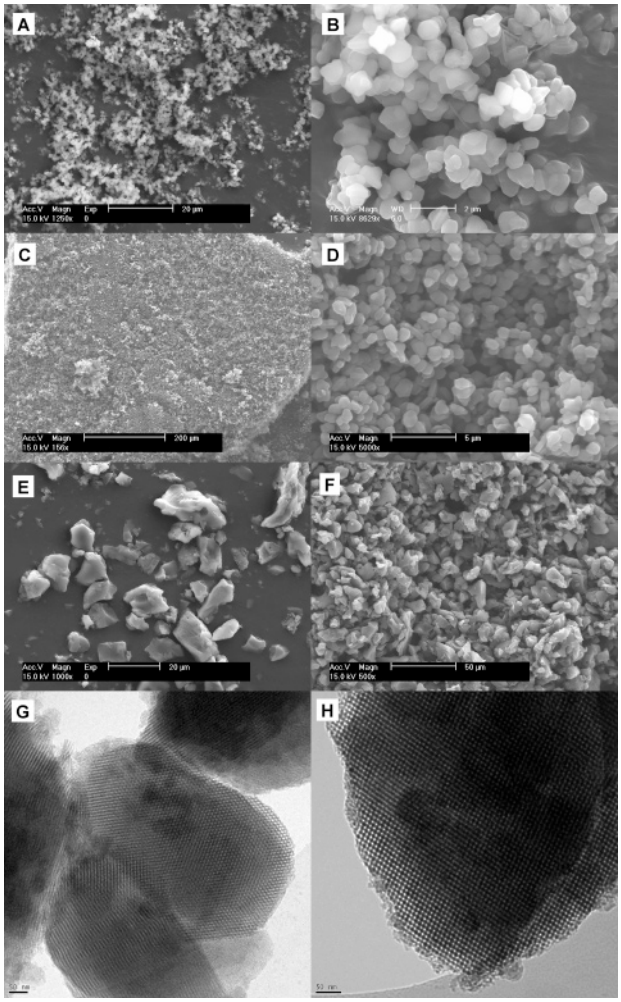

Figure 2. SEM images of powdery SBA-15 ((A) in low magnification and (B) in high magnification), monolithic SBA-15M ((C) in low magnification and (D) in high magnification), (E) powdery KIT-6, and (F) monolithic KIT-6M. TEM images of (G) SBA-15M and (H) KIT-6M.

Results and Discussion

Hierarchically Ordered Silica Monoliths. Figure 1 shows the typical photographs of powdery mesoporous silicas, silica monolith, and carbon monoliths. When proper glass vials with different inner diameters are chosen, silica monoliths and carbon monoliths with various sizes can be easily achieved. In this study, carbon monoliths have been made with (but are not limited to) a diameter up to 1 cm and a length up to 8 cm. It should be noted that the dimensions of the silica monoliths and thereof nanocasted carbon monoliths are not constrained by the method used in this work, but are instead limited by the geometry of the centrifuge holders.

As shown in Figure 2, mesoporous silica monoliths exhibit similar primary particles with comparable sizes to their

(22) Kruk, M.; Jaroniec, M.; Gadkaree, K. P. *J. Colloid Interface Sci.* **1997**, *192*, 250.

(23) Thrower, P. A. *Materials in Today's World*, 2nd ed.; McGraw-Hill: New York, 1995; p 87.

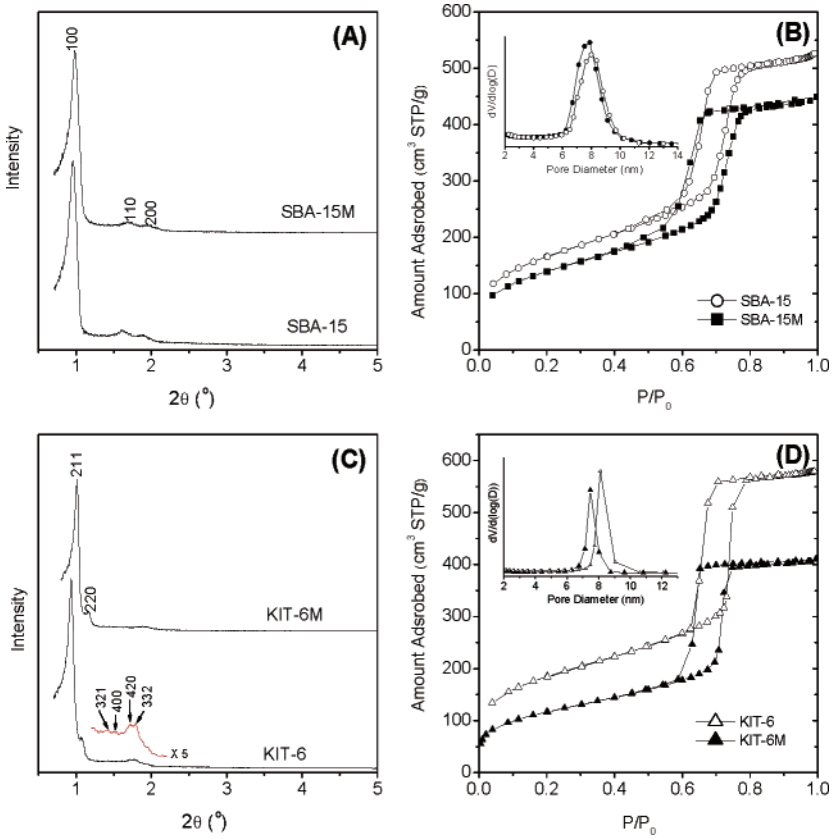

Figure 3. XRD patterns (A and C) and N_2 sorption isotherms (B and D) of mesoporous silicas in the forms of powder (obtained after calcination at 550 °C) and monolith (after being sintered at 700 °C). Inserts (in B and D) are the BJH pore size distribution plots.

powdery counterparts. Unlike individual particles in the powder form, micrometer-sized primary silica particles are fused with neighbors to form a monolith during sintering at high temperature. Thus, a rigid 3D interconnected silica network is generated with observable macroporosity generated by the removal of organic polymer. XRD patterns and N_2 sorption isotherms of powdery and monolithic mesoporous silicas are shown in Figure 3. After being sintered at 700 °C, SBA-15M and KIT-6M retain highly ordered hexagonal and cubic structure, respectively, as evidenced by the well-indexed peaks in XRD patterns and TEM images (Figures 2G and 2H). However, the unit cell of silica monoliths shrinks slightly with a decrease in surface area, pore size, and pore volume, which can be attributed to the formation of compacted structures at high temperature. In addition, N_2 sorption isotherms of monolithic silicas (both SBA-15M and KIT-6M), analogous to those of powdery silicas, show capillary condensation at medium relative pressures with an H2-type hysteresis. There is no obvious adsorption of N_2 at high relative pressure (e.g., $P/P_0 > 0.8$), indicating the absence of additional interparticle mesoporosity. It was found that mesoporous silicas templated by block copolymers under acidic conditions inherently possess microporosity within the silica wall,[24] which allows connections between adjacent carbon nanorods or nanopipes and ensures interconnected carbon inverse replicas after removal of the silica template (Scheme 1). Although pore volume decreases after being sintered at high temperature, both of the monolithic silica samples still exhibit some microporosity and are therefore suitable as hard templates to prepare ordered mesoporous carbon monoliths. Structural properties of the mesoporous silicas are summarized in Table 1. For comparison, mesoporous silica monoliths of "reference" samples were made by the same procedure but without the aid of the organic gel. After centrifugation of the aqueous suspension of mesoporous silica powders into molds, wet monoliths were formed. However, the monoliths cracked during the drying process and the monolithic morphology was further destroyed after being sintered at 700 °C. Therefore, the "reference" silica samples were not suitable for preparation of carbon monoliths.

Table 1. Structural Properties of Silica Templates[a]

sample	S_{BET} (m^2/g)	V_t (cm^3/g)	V_m (cm^3/g)	w_{BJH} (nm)	a (nm)
SBA-15	582	0.81	0.067	8.0	10.65
SBA-15M	492	0.69	0.054	7.9	10.36
KIT-6	634	0.90	0.112	8.1	23.07
KIT-6M	407	0.64	0.048	7.5	21.52

[a] S_{BET}: BET surface area; V_t: total pore volume; V_m: micropore volume; w_{BJH}: the maximum of BJH pore size distribution peak; a: unit cell parameter.

Ordered Carbon−Silica Composites and Carbon Monoliths and Effects of Carbon Precursor Concentrations. Liquid furfuryl alcohol (FA) is selected as a carbon precursor because it can be well-impregnated into the pores of silica template and easily polymerized in the presence of oxalic

(24) Joo, S. H.; Ryoo, R.; Kruk, M.; Jaroniec, M. *J. Phys. Chem. B* **2002**, *106*, 4640.

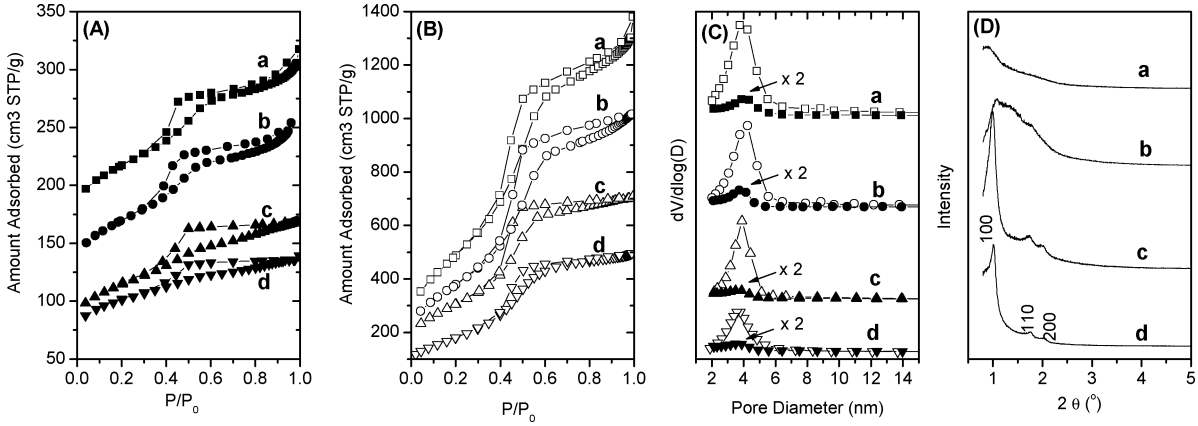

Figure 4. N_2 sorption isotherms of (A) carbon−silica composites SC-15-*X* and (B) carbons C-15-*X*. (C) BJH pore size distribution plots (solid symbol: composites; open symbol: carbons). (D) XRD patterns of carbons C-15-*X*. *X* = 30 (a), 40 (b), 60 (c), and 80 (d).

Table 2. Structural Properties of Carbons C-15-*X*[a]

sample	S_{BET} (m^2/g)	V_t (cm^3/g)	V_m (cm^3/g)	w_{BJH} (nm)	*a* (nm)
C-15-30	1783	2.13	0.42	3.78	disordered
C-15-40	1368	1.57	0.28	4.24	disordered
C-15-60	1078	1.10	0.22	3.89	10.2
C-15-80	875	0.76	0.15	3.79	9.9

[a] See notes in Table 1.

acid (OxA).[25] To nanocast from silica monoliths, the amount of carbon filled into the mesopores of templates must be carefully controlled. Enough carbon precursor should be used to replicate the mesostructures of silica templates and also maintain the whole monolithlic structural integrity, but if too much is used, formation of unwanted disordered carbons may occur.[17b] Therefore, to regulate the amount of carbon incorporated, silica monoliths were immersed in a series of FA solutions at different concentrations in trimethylbenzene (TMB) containing OxA (molar ratio of FA/OxA = 250). After polymerization and carbonization of FA, the resulting silica−carbon composites and carbon monoliths, obtained by dissolving silica templates by HF, from monolithic SBA-15M are referred as SC-15-*X* and C-15-*X*, respectively, where *X* is the vol % of FA in TMB. Figures 4A and 4B show the N_2 sorption isotherms of SC-15-*X* and C-15-*X* prepared from FA solutions with various concentrations. There is a clear trend that, with the increase of concentration of FA, increased amounts of carbon are gradually filled into the pores of silica templates, as indicated by a decrease in N_2 adsorption on both silica−carbon composites and carbon monoliths. Figure 4D shows the XRD patterns of carbon materials after removal of SBA-15M. Structural properties of C-15-*X* are summarized in Table 2. Carbon materials prepared from low FA concentrations, C-15-30 and C-15-40, show one broad XRD peak, indicating a poor structural order, even though they exhibit typical IV N_2 adsorption isotherms with uniform pore size. This is believed to be a result of structural loss after removal of silica templates due to insufficient amounts of impregnated carbon. In comparison, carbon monoliths prepared with 60 and 80 vol % of FA in TMB, C-15-60 and C-15-80, exhibit uniform pore size and well-resolved XRD peaks which can be indexed into 100, 110, and 200 reflections of the 2D hexagonal symmetry group (*p6mm*), analogous to the parent SBA-15M. In addition, C-15-30 and C-15-40 should be carefully dried to keep the monolithic morphology, but sometimes cracks can still be found in the monoliths. However, carbon monoliths made from high FA concentrations exhibit excellent structural integrity and thus stronger mechanical stability. All of the above results suggest that highly ordered mesoporous carbon monoliths could only be obtained with sufficient carbon impregnated into the ordered mesopores of monolithic silica templates.

Figure 5 shows the SEM images of carbon−silica composite SC-15-60 and monolithic carbon C-15-60. Both of them exhibit the 3D connected network containing micrometer-sized primary particles with similar particle size and morphology to those of parent silica template SBA-15M, as shown in Figures 2C and 2D. Macroporosity still remains after carbonization and removal of the silica template. In ref 17b it is shown that when too much carbon precursor was used, irregular carbon particles formed in the macropores during preparation of carbon monolith. In our experiments, we used different FA concentrations (30%, 40%, 60%, and 80%) and found that 60% is better than 80% in terms of the amount of disordered carbon, as observed by SEM. The TEM image of C-15-60 (Figure 6) reveals a highly ordered hexagonal structure, which is the inverse replica of SBA-15. It is clear that carbon monoliths positively resemble the macroscopic morphology of the silica templates but negatively replicate their structures at the nanoscale.

Accordingly, carbon monoliths with cubic mesostructures can be made from monolithic KIT-6M with cubic *Ia3d* symmetry. Figure 7 shows N_2 sorption isotherms, BJH pore size distribution plots, and XRD patterns of monolithic carbons prepared from various concentrations of FA (containing oxalic acid with molar ratio of FA/OxA = 250) in TMB using KIT-6M as the silica template. Similarly, the resulting monolithic carbons exhibit well-resolved XRD peaks, which can be indexed to 211 and 220 reflections assuming the cubic *Ia3d* symmetry group, same as that of parent silica monolith KIT-6M (Figure 7B). Unlike in the case of C-15-40, carbon monolith prepared with 40 vol % of FA maintains highly ordered cubic structure of KIT-6M.

(25) (a) Lu, A.-H.; Schmidt, W.; Spliethoff, B.; Schüth, F. *Adv. Mater.* **2003**, *15*, 1602. (b) Lu, A.-H.; Li, W.-C.; Schmidt, W.; Schüth, F. *Microporous Mesoporous Mater.* **2005**, *80*, 117.

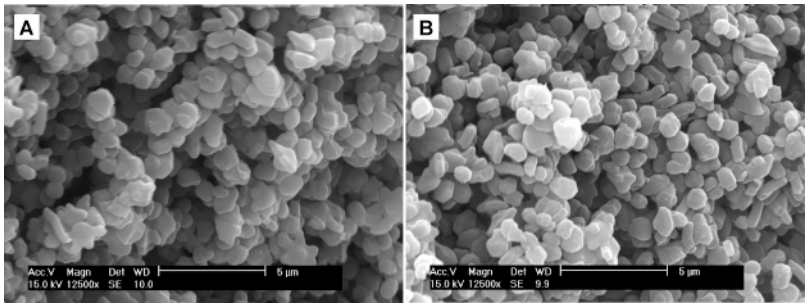

Figure 5. SEM images of (A) silica−carbon composite SC-15-60 and (B) carbon monolith C-15-60.

Figure 6. TEM image of carbon monolith, C-15-60, with a hexagonal mesostructure.

The unique bicontinuous cubic pore structure of KIT-6 could likely facilitate the enhancement of the connectivity of the resulting carbons and therefore keep the structural integrity of cubic carbon monoliths both macroscopically and at the nanoscale.

Control of Meso- and Microporosity in Carbon−Silica Composites and Carbon Monoliths by Chemical Vapor Deposition. As shown in Table 2, the carbon monoliths are highly microporous, which is inherent for mesoporous carbon materials made from sucrose or furfuryl alcohol by the wet impregnation method as a consequence of carbonization at high temperature and removal of the silica template.[26] On the other hand, as reported by Xia and Mokaya,[27] ordered mesoporous carbons fabricated via gas-phase chemical vapor deposition (CVD) exhibited less or no microporosity. Further advantages of the CVD method include the fact that resulting carbon materials possess graphitic pore walls, and that it is feasible to prepare N-doped carbon materials with a polar nature[28] when acetonitrile is used as the carbon precursor.

Unlike the work of Xia and Mokaya in which pure siliceous mesoporous materials were used (e.g., SBA-15), herein we use silica−carbon composite, SC-15-10, as the solid template. Compared to pure siliceous SBA-15, SBA-15-carbon composite exhibits more hydrophobic properties and is therefore likely to facilitate sufficient impregnation of carbon into the micro- and mesopores of the hard template. During the CVD process, acetonitrile was pyrolyzed and filled into the pores of the silica−carbon composite. As illustrated by the N_2 sorption isotherms shown in Figure 8A, with the increase in the CVD temperature, the resulting silica−carbon composites show decreasing N_2 adsorption capacity. At 750 °C, the obtained composite exhibits a typical IV type N_2 adsorption isotherm with narrow pore size distribution, similar to that observed for the composites[29] when preparing tubelike CMK-5 under vacuum. There is a clear N_2 adsorption step starting at $p/p_0 = 0.4$, a shift to lower relative pressure compared to that found for SC-15-10. In addition, all composites obtained after the CVD process exhibit no detectable microporosity. The results indicate a gradual impregnation of carbon into the micropores and then into the mesopores of the template.

Removal of the silica template from CVD-treated SC-15-10 at 750 °C results in the formation of tubelike CMK-5, as indicated by N_2 sorption analysis and relatively high intensity of the 110 peak in the XRD pattern (Figure 8D). However, cracks formed during drying after dissolution of the silica template because of an insufficient amount of impregnated carbon to maintain the monolithic morphology. As the CVD temperature increases to 800 °C, the composite obtained exhibits very low N_2 uptake, suggesting complete filling of carbon into the micro- and mesopores of the templates at high temperatures. The higher CVD temperatures lead to the lower surface areas of both composites and the related carbon materials but higher structural order, as shown in XRD patterns (Figure 8D). Compared to CMK-5 obtained at 750 °C, high CVD temperatures (e.g., >800 °C) result in the formation of monolithic CMK-3 without cracks and with no accessible microporosity. These interesting properties ensure such monolithic carbon materials will be good candidates as stationary phases for monolithic high-performance liquid chromatography (HPLC). Textural properties of both composites and carbon materials obtained from the SBA-15-carbon composite, SC-15-10, after deposition of acetonitrile at different temperatures, are summarized in Table 3.

Inspired by the above results, a similar CVD process was performed at 800 °C for 2 h using a composite (denoted as SC-15L-10), which was prepared with 10 vol % FA in TMB from monolithic SBA-15 with larger mesopore size, as the hard template. After removal of silica template, the resulting carbon retains the monolithic morphology without any

(26) Choi, M.; Ryoo, R. *Nat. Mater.* **2003**, *2*, 473.
(27) (a) Xia, Y.; Mokaya, R. *Adv. Mater.* **2004**, *16*, 886. (b) Xia, Y.; Mokaya, R. *Chem. Mater.* **2005**, *17*, 1553.
(28) Hou, P.-X.; Orikasa, H.; Yamazaki, T.; Matsuoka, K.; Tomita, A.; Setoyama, N.; Fukushima, Y.; Kyotani, T. *Chem. Mater.* **2005**, *17*, 5187.
(29) Kurk, M.; Jaroniec, M.; Kim, T.-W.; Ryoo, R. *Chem. Mater.* **2003**, *15*, 2815.

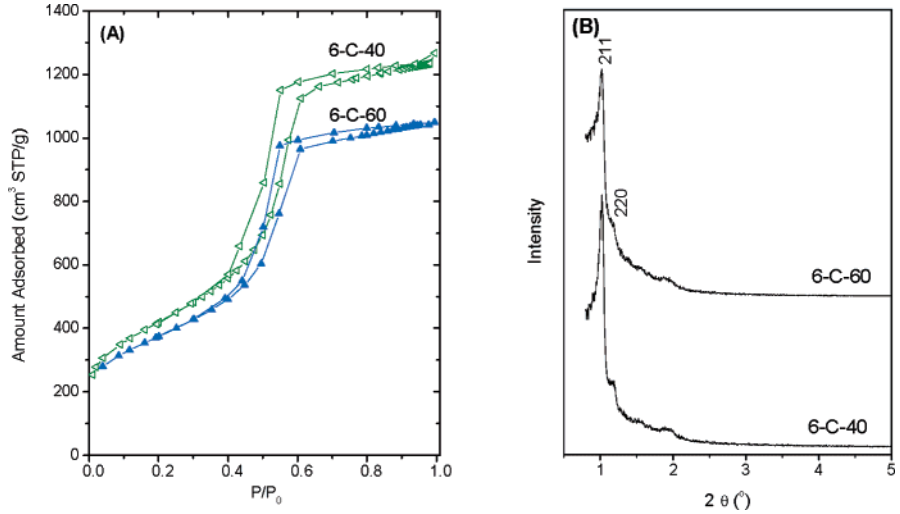

Figure 7. (A) N_2 sorption isotherms and (B) XRD patterns of carbon monoliths obtained from monolithic KIT-6M and various concentrations of FA in TMB.

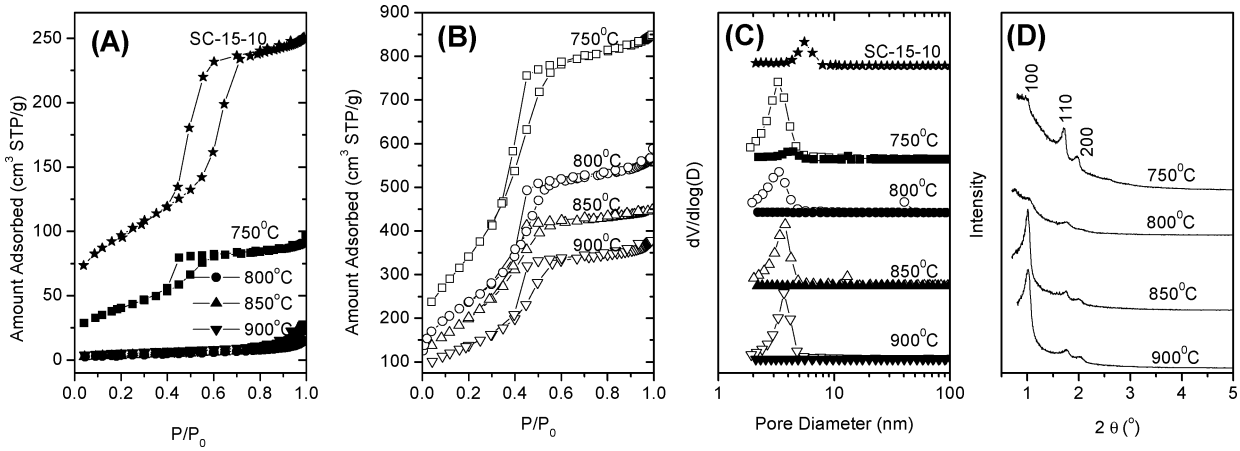

Figure 8. N_2 sorption isotherms of (A) SC-15-10 and carbon−silica composites obtained after CVD at different temperatures for 3 h and (B) the related carbons after removal of the silica templates. (C) BJH pore size distribution plots (solid symbol: composites; open symbol: carbons). (D) XRD patterns of carbons.

Table 3. Structural Properties of Both Composites and Carbon Materials Obtained from SC-15-10 after Deposition of Acetonitrile at Different Temperatures[a]

CVD temp (°C)	sample	S_{BET} (m^2/g)	V_t (cm^3/g)	V_m (cm^3/g)	w_{BJH} (nm)	a (nm)
	SC-15-10	334	0.39	0.032	5.52	8.80
750	composite	145	0.17	0	4.43	
	carbon	1303	1.31	0	3.37 (+shoulder)	8.80
800	composite	14.2	0.02	0		
	carbon	766	0.72	0	3.34	8.78
850	composite	13.4	0.03	0		
	carbon	684	0.69	0	3.49	8.76
900	composite	11.2	0.02	0		
	carbon	602	0.58	0	3.68	8.71

[a] See notes in Table 1.

Table 4. Compressive Strengths of Monolithic Materials

sample[a]	compressive strength[b] (psi)	sample[a]	compressive strength[b] (psi)
SBA-15M	36.0	C-6-60	20.6
SC-15-10	51.0	SBA-15LM	29.7
CMK-3M	22.7	CMK-5M	9.5
KIT-6M	27.9		

[a] CMK-3M: obtained by CVD treatment of SC-15-10 at 900 °C for 3 h; C-6-60: obtained from 60% FA using KIT-6M as template; SBA-15LM: made from large-pore SBA-15; CMK-5M: obtained by CVD treatment of SC-15L-10 at 800 °C for 2 h. [b] 1 psi = 6890 Pa.

cracks. The XRD pattern (Figure 9C) shows five well-resolved peaks, which can be indexed as 100, 110, 200, 210, and 300 reflections from the hexagonal *p6mm* symmetry group. The relative high intensity of the 110 peak indicates the formation of monolithic CMK-5 with tubelike structures (CMK-5M).[7,29,30] Figure 10 shows the high-resolution TEM images of CMK-5M along the [001] and [110] directions. Cleary, hexagonally packed circles are visible along the channel direction and a parallel pattern of dark lines is observed perpendicular to the channel direction. The BET surface area of CMK-5M is calculated to be 739 m^2/g from the N_2 adsorption isotherm (Figure 9A(c)), much smaller than that observed for CMK-5 reported previously, attributable to the lower microporosity and the thicker tube walls for CMK-5M (2.5 nm estimated from TEM image) than for

(30) (a) Solovyov, L. A.; Kim, T.-W.; Kleitz, F.; Terasaki, O.; Ryoo, R. *Chem. Mater.* **2004**, *16*, 2274. (b) Zhang, W.-H.; Liang, C.; Sun, H.; Shen, Z.; Guan, Y.; Ying, P.; Li, C. *Adv. Mater.* **2002**, *14*, 1776.

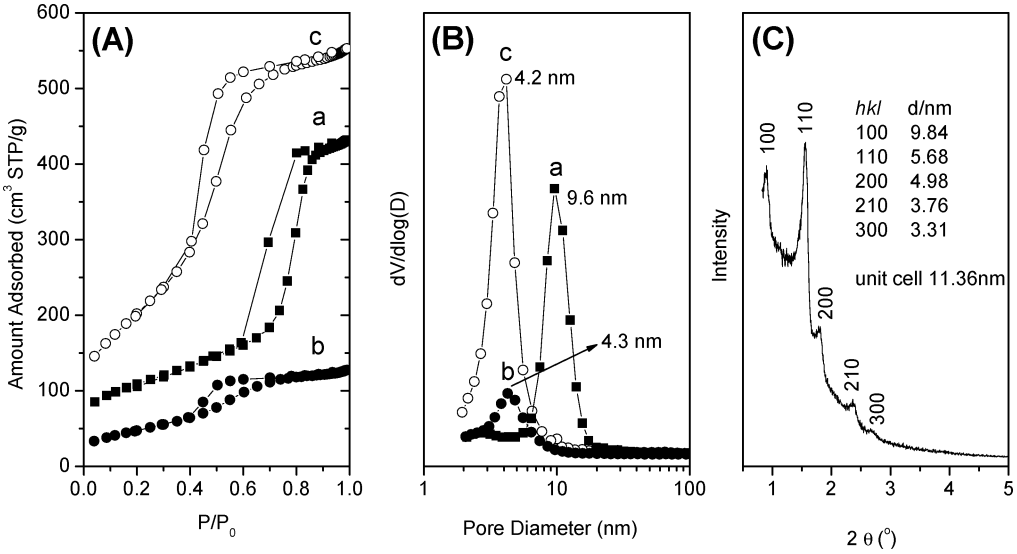

Figure 9. (A) N_2 sorption isotherms and (B) BJH pore size distribution plots of SC-15L-10 (a), the composite obtained after CVD process at 800 °C for 2 h (b), and CMK-5M after removal of template (c). (C) XRD pattern of CMK-5M.

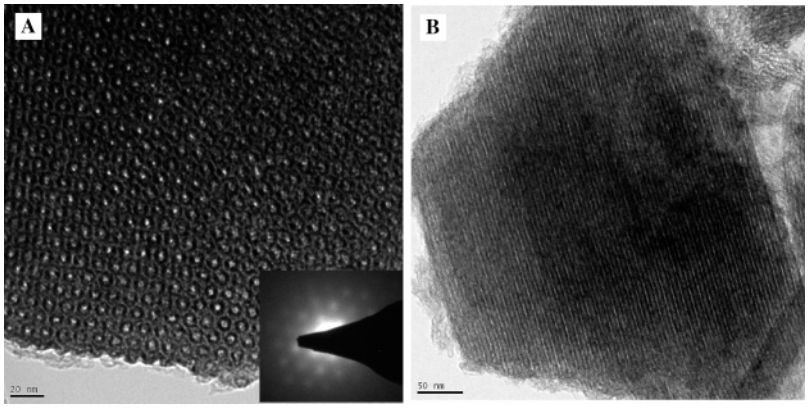

Figure 10. TEM images of CMK-5M along the [001] (right, the insert is the electron diffraction pattern) and [110] (left) directions.

conventional CMK-5 powder (around 1 nm).[30a] Other factors, for example, the pore blocking and the formation of amorphous carbon on the external surface of the particles, might also be responsible for the small surface area of CMK-5M. Both pore sizes between tubes and inside tubes are around 4.2 nm (Figure 9B). To the best of our knowledge, this is the first report of hierarchically porous monolithic carbon with hexagonal tubelike mesostructure.

Energy-dispersive X-ray (EDX) analysis was carried out for all carbon materials after removal of the silica templates. The results show less than 2 wt % of silica remained, revealing the monoliths are constructed free of template.

Mechanical Properties. To evaluate the mechanical strength of monolithic materials, the compressive strength, the compressive force per unit area that a material can withstand, was measured. The compressive strength of monolithic SBA-15M was 36 psi, and it increased to 51 psi after incorporation of 10% FA (SC-15-10). However, monolithic CMK-3, obtained by CVD treatment of SC-15-10 at 900 °C for 3 h and subsequent removal of the silica template, exhibited less strength (22.7 psi), which is probably due to the formation of defects after removal of the silica template. Results of the compressive strength of other monolithic materials are listed in Table 4.

Conclusion

We have described a facile synthetic procedure to prepare hierarchically porous carbon monoliths with ordered mesostructures from powdery mesoporous silicas, hexagonal SBA-15 and cubic KIT-6. Carbon monoliths with highly ordered mesostructures and good morphology integrity can be made by a second impregnation of carbon by the CVD method. With control of the CVD temperature, carbon monoliths constructed from both rod-type (CMK-3) and tubelike (CMK-5) mesostructures have been fabricated from powdery SBA-15. Preliminary mechanical strength results indicate that such materials are rigid. The method can be extended to make other hierarchically porous carbon monoliths with ordered meso- or microstructures because the template silica monoliths can be made with readily available porous silica powder. Hierarchically porous carbon monoliths coupled with ordered

(31) Liang, C.; Dai, S.; Guiochon, G. *Anal. Chem.* **2003**, *75*, 4904.
(32) (a) Lee, J.; Yoon, S.; Hyeon, T.; Oh, S. M.; Kim, K. B. *Chem. Commun.* **1999**, 2177. (b) Lee, J.; Yoon, S.; Oh, S. M.; Shin, C. H.; Hyeon, T. *Adv. Mater.* **2000**, *12*, 359.
(33) Zhou, H.; Zhu, S.; Hibino, M.; Honma, I.; Ichihara, M. *Adv. Mater.* **2003**, *15*, 2107.

mesoporosity, tunable microporosity, and surface properties have potential applications in monolithic HPLC,[31] electrochemical doubly layered capacitor (EDLC),[32] and advanced electrodes.[33] In addition, surface functionalization of these carbon monoliths via chemical[34] or electrochemical[35] pathways can be readily achieved to custom tailor them for specific needs in a wide range of important applications.

Acknowledgment. This work was partially supported by the NSF and Beckman Foundation. P.F. is a Camille Dreyfus Teacher-Scholar.

Supporting Information Available: A detailed description and a scheme of the compressive strength tests (PDF). This material is available free of charge via the Internet at http://pubs.acs.org.

CM061531A

(34) (a) Li, Z. J.; Dai, S. *Chem. Mater.* **2005**, *17*, 1717. (b) Li, Z. J.; Yan, W.; Dai, S. *Langmuir* **2005**, *17*, 1553.

(35) (a) Delamar, M.; Hitmi, R.; Pinson, J.; Savéant, J. M. *J. Am. Chem. Soc.* **1992**, *114*, 5883. (b) Bahr, J. L.; Tour, J. M. *Chem. Mater.* **2001**, *13*, 3823. (c) Hudson, J. L.; Casavant, M. J.; Tour, J. M. *J. Am. Chem. Soc.* **2004**, *126*, 11158.